c) REMARKS

The claims are 44-48 and 51-62 with claims 44, 53 and 54 being independent. New dependent claims 55-62 have been added. Claims 55 and 56 are supported on page 13 and 20, for example. Claims 57-62 correspond to former Claims 45-48, 51 and 52, respectively.

Claims 44-48, 51, 52 and 54 were rejected as obvious over Ozin '666 in view of Kato '579. Claim 53 was rejected as obvious over Ozin in view of Mishina '539.

Claims 44-48 and 52 were also rejected as an obviousness-type double patenting over claim 1 of Kuroda '546 in view of Kato '579. Claim 51 was rejected as an obviousness-type double patenting over claim 1 of Kuroda in view of Kato and Ozin. Claim 53 was deemed an obviousness-type double patenting over claim 1 of Kuroda in view of Mishina.

The grounds of rejection are respectfully traversed. Prior to addressing the grounds of rejection applicant wishes to briefly review certain key features and advantages of the present claimed invention.

The present invention relates to a porous structure and has a feature that full width at a half maximum of the normal distribution is about 35° or less. This feature is obtained by the present invention which includes a first portion containing a polymer having oriented polymer chains and the polymer having a sequence of at least two adjacent methylene groups and at least one imide bond in the repeating unit; or a first portion containing polyimide having oriented polyimide chains and the polyimide having a sequence of at least two adjacent methylene groups in the repeating unit. This feature makes it possible to provide a structure having uniaxially oriented pores with high

regularity, whereby the structure is readily adapted for use in an optical device or an electronic device.

Regarding the art rejection, Ozin '666 relates to a light-emitting device. Ozin discloses that a porous structure is formed in a polyethylene vessel, and that the pores are oriented in parallel to a substrate. Kato discloses that an oriented film for use in a liquid crystal employs a polymer having a sequence of two or more methylene groups and at least one imide bond in the repeating unit. Minami discloses an oriented film for use in a liquid crystal. Minami also discloses use of a polymer having a sequence of two or more methylene groups and at least one imide bond in the repeating unit. Applicant will show there is no motivation to combine the references and, even if combined, a *prima facie* case of obviousness is not obtained.

The primary reference, Ozin, discloses a film different in kind from the claimed invention. In order to aid the Examiner in understanding the difference between conventional X-ray diffraction and in-plane X-ray diffraction (XDR), discussed hereafter, applicant has attached Exhibits 3 and 4 as follows:

Exhibit 3 – Measured results of in-plane XDR (half width value = 12.6°);

Exhibit 4 – Explanation of X-ray diffraction (Conventional diffraction vs. in-plane diffraction).

Conventional diffraction is used for determining arrangement of pores on a section, and in-plane diffraction is used for determining arrangement of pores in one axis direction from a top view. The horizontal section and vertical section of a film of the present invention and a film of Ozin are schematically shown in Exhibit 1, attached, having Figs. A, B, C and D, respectively. The vertical section of Fig. C, showing the sectional

structure of the present invention, is similar to the vertical section of Fig. D, showing the sectional structure of Ozin. However, Fig. A of the present invention should be compared to Fig. B of Ozin '666. Fig. A and B are horizontal sections from a top view. In Fig. A the tubular pores in the film of the present invention are regularly aligned in a uniaxial orientation direction. In Fig. B the tubular pores in the film of Ozin are not aligned in an uniaxial orientation direction. This shows that regularity cannot be obtained by measuring a normal distribution of the film of Ozin.

The reason why the film of Ozin exhibits the wavy structure of Fig. B is described below. Ozin, et al. have published a paper entitled "Free-standing mesoporous silica film; morphogenesis of channel and surface patterns" J. Mater. Chem., 1997, 7(9), 1755-1761 attached as Exhibit 2. In that paper, a solution for forming a porous structure is charged in a polyethylene vessel and the porous structure is formed within the vessel. Although the experimental conditions of the paper are slightly different from those of Ozin '666 patent, this does not influence the resulting orientation of the pores and, therefore, the film formed in the Ozin, et al. paper is the same as the film disclosed by the Ozin '666 patent.

Ozin's paper discloses that an oriented mesoporous silica film is synthesized. The word "oriented " used in the paper has the same meaning as used in the Ozin patent. The word "oriented" means regularity of pores taken from a vertical section. That is, it refers to the oriented state of Fig. D. of Exhibit 1. However, it is clear from Fig. 2 of the Ozin paper on page 1757 that the tubular pores form a wavy pattern on a horizontal section as seen from a top view. This is illustrated in Fig. B of Exhibit 1. The Ozin paper states on page 1756, right column, lines 4 to 9 that: "the channels contained within each

domain are oriented parallel to the film surface. However, the channels do not exist in a uniform collinear arrangement within the domains." This observed result shows that Ozin's tubular pores are not uniaxially oriented. This is confirmed in the Ozin paper's "Conclusion" on page 1761 in which the channel patterns are said to be circles, herringbones, fingerprints and hairpins . . . and . . . patterns that appear to reflect Channel curvature designs within the film. Accordingly, Ozin's film does not have the feature of the present invention that full width at a half maximum of the normal distribution is about 35° or less.

Finally, Ozin uses a polyethylene vessel only as a vessel for forming a film. In the experimental system of water-heat synthesis, a plastic vessel is usually used and, therefore, use of a plastic vessel has no disclosed consequence. As described in the above explanation of Ozin, polyethylene as a polymer in Ozin, is merely used as a mold of a vessel. It is not suggested that ethylene has an influence on the formation conditions of a porous structure. To change the formation conditions for a porous structure, Ozin changes the composition of a solution and temperature, but Ozin does not change the material of the vessel. That is; Ozin fails to teach or suggest applying an oriented film to a vessel, itself, made of a polyethylene as a polymer for any specific advantage.

The defects of Ozin are not remedied by Kato or Minami. Kato and Minami each disclose an oriented film for use in a liquid crystal. They also disclose that a polymer of the oriented film is a polymer having a sequence of at least two methylene groups and at least one imide bond in the repeating unit of the polymer. The Examiner asserts that it would have been obvious to combine Kato or Minami with Ozin. However, it would not have been obvious for a skilled person to combine Ozin's method of forming a film for use

in a light-emitting device with Kato or Minami, which concern using an oriented film in a liquid crystal display. Further, the resulting combination would not achieve the orientation of pores of the present invention.

With regard to the double-patenting rejection, the present claimed invention provides a structure having regular pores different to that of Kuroda '546. The claims of the present application define an improved polymer providing regularity of pores and therefore are not obvious over the claims of Kuroda. Kuroda also fails to claim the instant polymide or that the tubular pores are aligned with a normal distribution, full width at a half maximum of the normal distribution being about 35° or less.

The claims should be allowed and the case passed to issue.

Applicant's undersigned attorney may be reached in our New York office by telephone at (212) 218-2100. All correspondence should continue to be directed to our below listed address.

Respectfully submitted,

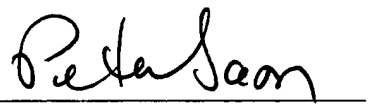

Peter Saxon
Attorney for Applicant
Registration No. 24,947

FITZPATRICK, CELLA, HARPER & SCINTO
30 Rockefeller Plaza
New York, New York 10112-3801
Facsimile: (212) 218-2200

NY_MAIN 530142v1

EXHIBIT 1

Present invention

Ozin '666

Horizontal section

FIG. A

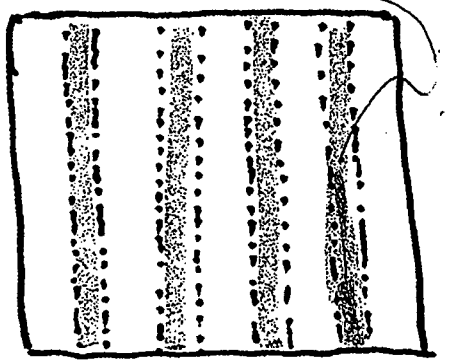

FIG. B

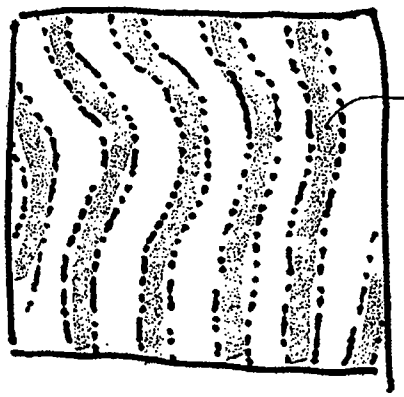

Vertical section

FIG. C

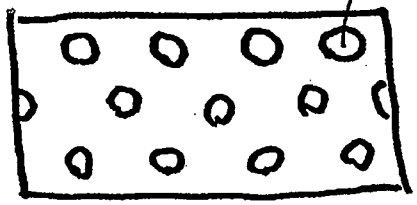

FIG. D

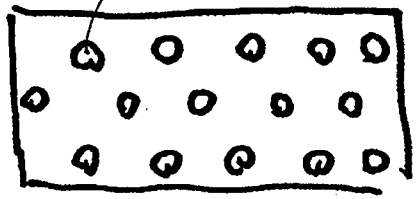

EXHIBIT 2

Free-standing mesoporous silica films; morphogenesis of channel and surface patterns

Hong Yang,[a] Neil Coombs,[b] Ömer Dag,[a] Igor Sokolov[a] and Geoffrey A. Ozin*[a]

[a]*Materials Chemistry Research Group, Chemistry Department, University of Toronto, 80 St. George St., Toronto, Ontario, Canada M5S 3H6*

[b]*Imagetek Analytical Imaging, 32 Manning Avenue, Toronto, Ontario, Canada M6J 2K4*

Extraordinary channel patterns have been observed in an oriented mesoporous silica film that is synthesized at the boundary between air and water. The basic channel designs comprise concentric circles, herringbones, fingerprints and hairpins. It is suggested that these patterns are spatio-temporal silicified recordings of the polymerization and growth of a silicate liquid-crystal seed emerging in two spatial dimensions at the air/water interface. The origin of the channel patterns may be from defects, such as disclinations and dislocations, that spontaneously form in a surface confined precursor silicate liquid-crystal film to give a liquid-crystalline texture to the resulting mesoporous silica film. The reaction–diffusion processes and defects that are believed to contribute to the curved three-dimensional morphologies and channel patterns of mesoporous silica free to grow in solution, may also occur in the surface version, except that the isotropy of solution is replaced by the anisotropy of the air/water interface together with proximity effects from neighboring growth centers. Polymerization induced radial stresses produced in the as-synthesized mesoporous silica film before drying, are relieved through warping of the film into micrometer-scale hillock-shaped protuberances. These mounds are arranged into patterns that appear to reflect the channel designs within the film. A linear radial stress model is found to successfully account for the warp patterns. A possible connection between the two-dimensional channel patterns in mesoporous silica films and the two-dimensional stripe domain patterns found in modulated phases is discussed.

Physical and chemical systems of a diverse kind have been found to exhibit patterns and shapes spanning microscopic to macroscopic length scales.[1] A particularly interesting example of a mesoscale pattern forming system involves the polymerization of silicate liquid-crystal phases. This process was shown by Mobil scientists to yield periodic mesoporous silicas.[2] The synthesis paradigm led to the assembly of free-standing hexagonal mesoporous silica films that emerge in the boundary region between air and water.[3] The channels in these films were established, by powder X-ray diffraction and transmission electron microscopy, to be oriented parallel to the air/water interface. Film growth was considered to involve collective interactions between polymerizable silicates, surfactant micelles and a surfactant overstructure all localized at the air/water interface.[3–6]

Although still the subject of debate, there is accumulating evidence that the formation of mesoporous silica involves sphere-to-rod micellar transitions in the presence of silicate to form a silicate liquid-crystal seed.[7] What is less obvious however, is how the seed polymerizes and evolves in size over three spatial dimensions in an aqueous environment. This question applies also to growth of the silicate liquid-crystal seed over two spatial dimensions when localized at planar interfaces. By definition, a liquid crystal is a mesophase which has partially or completely lost the long-range positional order of ordinary crystals, but possesses long-range orientational order of anisotropic structural units in one or more spatial dimensions. The essential criteria of the liquid-crystalline state are a certain degree of fluidity and, at the same time, some structural uniformity of the average alignment of the building blocks. Characteristic textures of liquid-crystal films are caused by the existence of various kinds of microscopic defects, such as disclinations and dislocations, that create distortion patterns of the director field.[8]

In this context, there is growing interest in the structure and spatial extent of the silicate liquid-crystal seed and how it relates to the genesis and form of mesoporous silica morphologies that grow in two and three spatial dimensions. Recent investigations of the pre-reaction stage in the assembly process, using cryo-transmission electron microscopy,[7] dynamic light scattering, and rheological techniques,[9] provided evidence for the existence of a *ca.* 50 nm silicate liquid-crystalline seed with a structure based on hexagonal packing of *ca.* 5 nm micelle rods.

In the experiments described here, we examine the spatio-temporal evolution of the silicate liquid seed when it is localized at the boundary between air and water. This process is compared to the circumstances where the seed is free to grow over all three spatial dimensions in an aqueous solution. It is demonstrated that an unusual class of patterns, traversing macro- and meso-scopic length scales, emerges for the mesoporous silica morphologies that grow in two spatial dimensions. It is interesting to consider whether the shapes, surface patterns, and channel plans recently documented for the mesoporous silica morphologies grown in solution[10] are related to the versions that concurrently appear at the surface of the solution.

Experimental

Synthesis

The synthesis of free-standing mesoporous silica films at the boundary between air and water utilized the following reactant mole ratios: 100 H_2O:7 HCl:0.11 CTACl:0.13 TEOS, where CTACl is the cationic surfactant $CH_3(CH_2)_{15}N(CH_3)_3Cl$ and TEOS is the silica source reagent $(C_2H_5O)_4Si$. The surfactant solution was mixed with TEOS and stirred for *ca.* 2 min at room temperature with a medium stirring speed and was then transferred to a polypropylene bottle. The solution was allowed to achieve a quiescent state and then left at 80 °C in an oven. After several minutes a film began to form at the air/water interface.

Characterization

Powder X-ray diffraction (PXRD) data were obtained on a Siemens D5000 diffractometer using Ni-filtered Cu-Kα radiation with $\lambda = 1.54178$ Å. A home-made plexiglass sample holder was used for recording the PXRD patterns. Samples for *in situ* VT-PXRD were prepared by lifting the free-standing

mesoporous silica film onto a Pt strip which was assembled onto the Pt hot stage of the diffractometer with the thermocouple located directly under the sample. The temperature ramp used was 4 °C min^{-1}. During the recording of PXRD patterns, the temperature was kept constant.

Transmission electron microscopy (TEM) and selected area electron diffraction (SAED) images were recorded on a Philips 430 microscope operating at an accelerating voltage of 100 kV. Specimens for TEM were prepared by carefully lifting the film, in a horizontal fashion from the aqueous side after growth periods of minutes to about one hour, onto either a pristine or a carbon-coated 400 mesh copper TEM grid. The films are thin enough for direct TEM imaging without any further treatment. SAED patterns were recorded from the film samples in the same microscope.

Atomic force microscopy (AFM) experiments were conducted on a NanoScope® III microscope (Digital Instruments, CA) using silicon-integrated tip cantilevers (Park Scientific Instruments, CA) for height mode scanning of the morphologies. The cantilevers were used as received. Images of the surfaces of the mesoporous silica were obtained by using direct contact (dc) scanning mode.

Optical microscopy images were recorded in transmission mode on an Olympus BH-2 microscope, using convergent white light.

Laser scanning confocal microscopy (LSCM) images of the films supported on a glass plate were recorded using a Bio-Rad 600 instrument in reflectance mode, with a 100 × objective using an Ar^+/Kr^+ 488 nm laser light source; the confocal arrangement rejects light from areas that are not in the focal plane and produces a true surface image.

Results and Discussion

A typical powder X-ray diffraction pattern of the film showed the presence of the (100) and (200) reflections characteristic of the hexagonal symmetry form of mesoporous silica, exhibiting preferred alignment of the channels with respect to the surface of the film.[3] Consistent with this PXRD-based model of the channel arrangement in the film are TEM images viewed orthogonally to the film along the [210] axis of the hexagonal unit cell, which show well defined parallel lines with a spacing of half that of the center-to-center distance between the channels.[3] A low magnification TEM image of a film grown for 3–5 min at the air/water interface shows a morphology comprised of roughly micrometer dimension domains with boundary walls and void spaces between them, Fig. 1. The inter

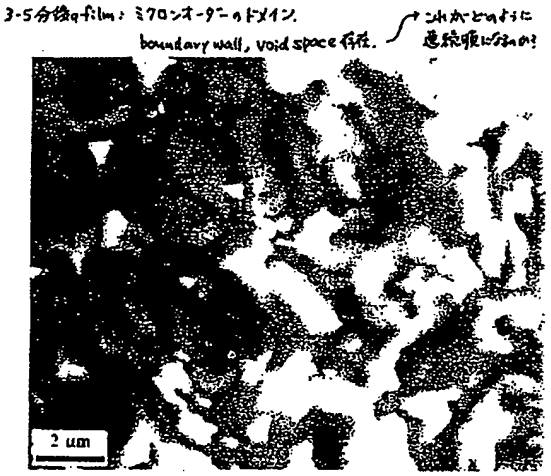

Fig. 1 TEM image showing the void spaces between domains in the mesoporous silica film grown at the air/water interface at an early growth stage

domain voids appear to be consolidated after *ca.* 10 min of film growth to create the impression of a continuous film.

Higher magnification TEM images of these samples reveal that the channels contained within each domain are oriented parallel to the film surface. However, the channels do not exist in a uniform collinear arrangement within the domains. Instead they form a continuum of striking swirling and curling channel patterns which, using descriptive names, can be roughly classified as concentric circles, herringbones, fingerprints and hairpins, Fig. 2.

An SAED study of the same samples used for the TEM imaging provides additional insight into the channel architecture of the film. It is found that when the diameter of the incident electron beam exposed to the film is gradually increased from 0.5 to 6 μm, the SAED pattern is seen to transform from the expected (210) and ($\bar{2}\bar{1}0$) sharp diffraction spots, corresponding to the *ca.* 25 Å center-to-center channel spacing, to an SAED pattern that displays increasing extents of streaking and arcing of the original two diffraction spots, to eventually form a discontinuous circle, Fig. 3. The SAED patterns maintain strict two-fold symmetry and are consistent with a polydomain film morphology, in which an increasingly large number of curved channels are placed within the area of the diffracted electron beam.

An optical micrograph of a mesoporous silica film grown at the air/water interface is shown in Fig. 4. The micrometer-scale stripe-like domain patterns running throughout the area of the film bear a resemblance to the spatial designs that are usually associated with modulated stripe phases found in diverse physical and chemical systems (see later).[11]

The as-synthesized mesoporous silica film formed at the air/water interface, at either room temperature or 80 °C, before and after drying is found to be crack-free. Interestingly, the film is seen to be deformed into intriguing micrometer-scale mounds that exclusively protrude away from the air/water interface. The topology of the film can be very effectively imaged by atomic force microscopy, Fig. 5, as well as laser scanning confocal microscopy, Fig. 6. The AFM images portray the overall topological landscape of the film, while the LSCM image displays contrast and optical interference patterns that emphasize the spatial variation in curvature across the film (see later).

The picture of the internal channel architecture of the mesoporous silica film that emerges from PXRD, TEM, SAED and LSCM studies is one of swirling and curling channel patterns that meander throughout the film, but with the channel axis strictly constrained to the plane that grows parallel to the air/water interface. Contraction induced radial stresses that build up during the growth process arise from the polymerization of silicate to silica in the interfacial region of the liquid-crystal template, and can be relieved through warping of the film (see later).

Growth model

In considering the likely sources of the channel patterns, it is assumed that the mesoporous silica film forming process begins with the assembly of ordered domains of a surfactant hemimicellar overstructure located at the air/water interface.[3–6] These assemblies may facilitate the formation of surface confined hexagonal silicate liquid-crystal seeds with the director field running predominantly parallel to the water surface. The growth of the seeds could proceed in a non-linear reaction–diffusion fashion in a far from equilibrium system,[1] with contributions from proximity (*i.e.*, frustration) effects arising from neighboring growth centers, to produce a film with domain patterns containing a maze of channels. The observed channel designs could emerge from defect induced patterns of the director field in a silicate liquid-crystal film that are quenched as a mesoporous silica facsimile.[8,12]

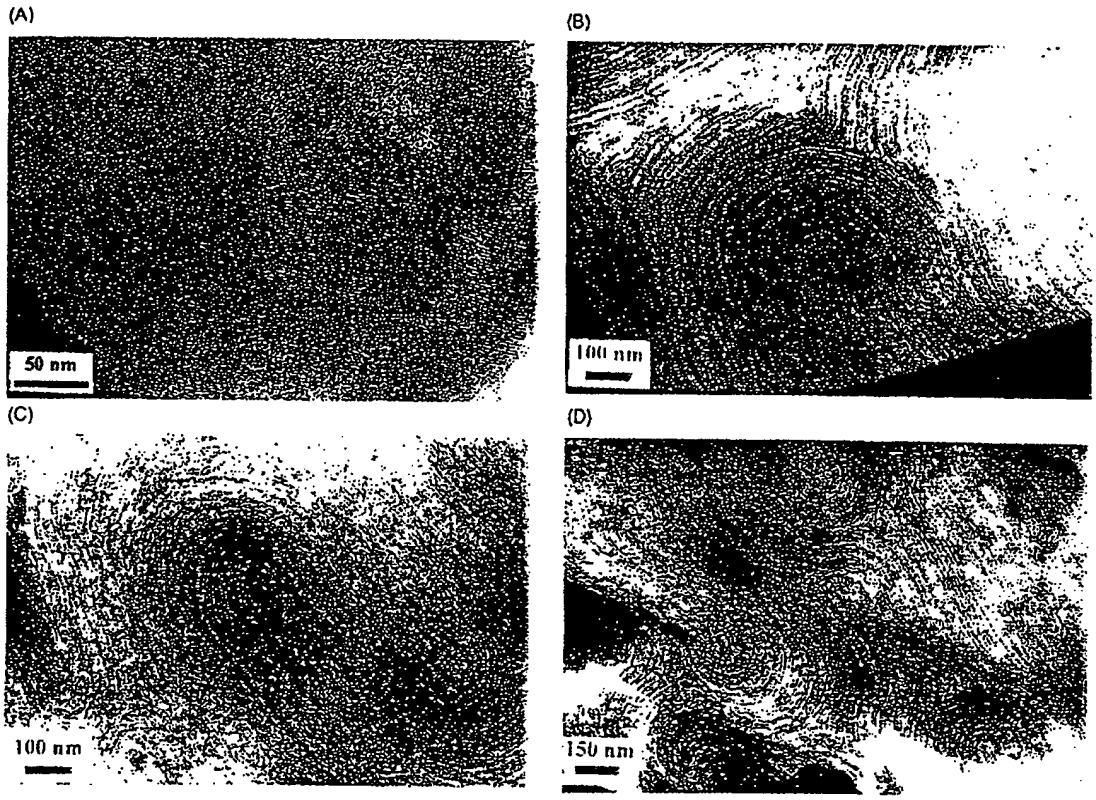

Fig. 2 Representative TEM images of the channel patterns for different areas of samples of mesoporous silica film grown at the boundary between air and water

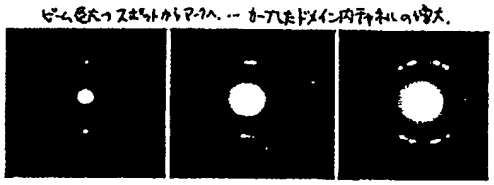

Fig. 3 SAED patterns of a mesoporous silica film grown at the boundary between air and water. Effective aperture diameters, left to right SAED patterns: 0.5 μm (spot), 1.5 μm (streaked), and 6 μm (arcs).

Before we probe further into these channel patterns, let us first briefly recap what is currently understood about the morphologies that are concurrently developing in the same synthesis solution where the silicate liquid-crystal seed is free to grow over three spatial dimensions.[10]

Mesoporous silica in three spatial dimensions

The various kinds of curved morphologies of mesoporous silicas grown under quiescent aqueous acidic conditions have recently been categorized into basic shapes ranging from ropes to toroids, discoids to gyroids, shells to spheroids.[10] The ropes typically have a curved and twisted body based upon an elongated hexagonal cylinder, display both arc and crankshaft body forms, show well defined faceting associated with abrupt body bending, and exhibit well formed hexagonal basal faces. The spatial relationship between the channel plan and the body shape of each mesoporous silica morphology was established by TEM. It is found that the channels that run down the body length of the ropes and wind around the toroids also run circumferentially about the discoids and gyroids. The mesostructure–morphology information implies that the basic mesoporous silica shapes are all related to the hexagonal cylindrical seed, which evolves into a family of inter-related forms, through the accretion of surfactant–silicate micelles and the concomitant development of increasing degrees of curvature.

These silica mesostructures are believed to appear from the condensation–polymerization of silicates organized in the head-group region of a hexagonal silicate liquid crystal, to create a silica copy of the templating interfaces. It is not obvious how the diffusion and reaction dynamics of a simultaneously polymerizing, accreting and enlarging surfactant–silicate embryo determine the final form of the mesoporous silica morphologies. The problem is compounded further because there do not exist any definite planes of lattice points and space patterns of

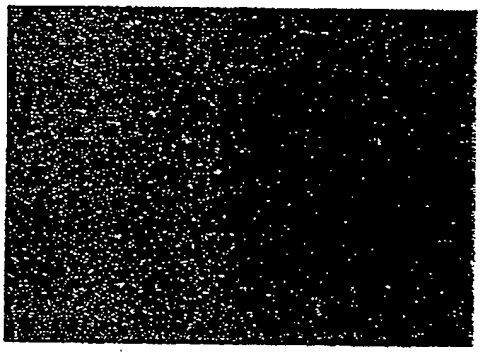

Fig. 4 An optical micrograph of a mesoporous silica film grown at 80 °C at the air–water interface, recorded in transmission mode using parallel polarized converging white light (image area: 700 × 930 μm)

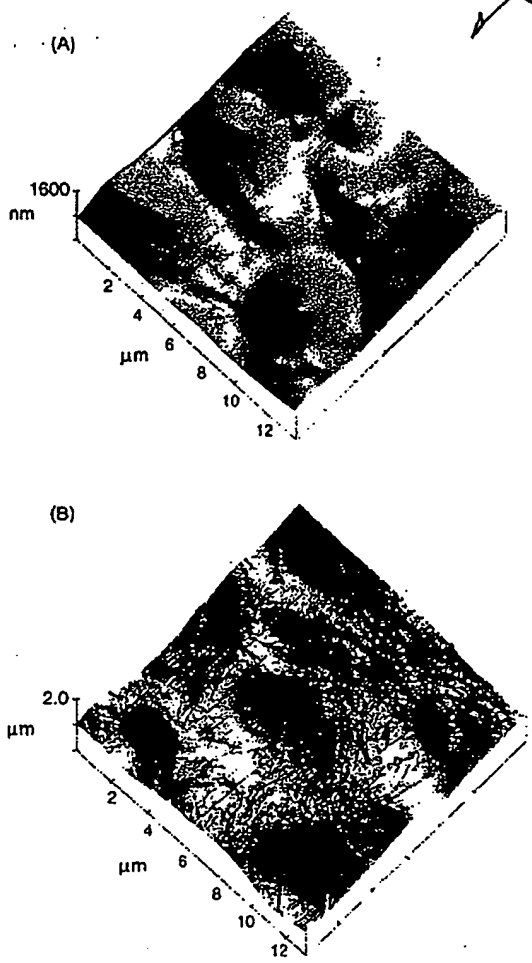

Fig. 5 AFM image showing the (A) top, and (B) bottom surface microtopography of a mesoporous silica film synthesized at the air/water interface

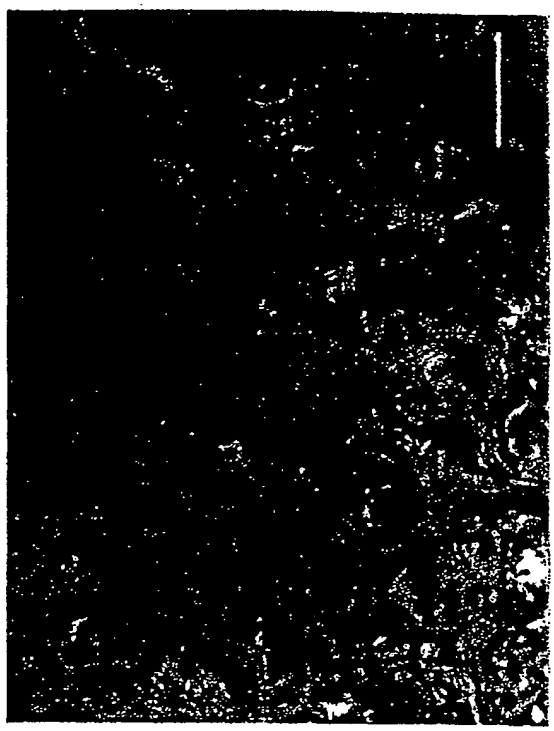

Fig. 6 LSCM image of a mesoporous silica film synthesized at the air/water interface (scale bar: 25 μm)

silicon and oxygen in these materials. Instead, the silica that constitutes the wall portions of the structure is disordered at the microscale but the channels are well ordered at the mesoscale. The morphologies of the mesoporous silicas synthesized in three spatial dimensions display a diversity of complex shapes, surface patterns and channel plans that are not typical for crystalline materials with polyhedral habits grown under equilibrium conditions.

It is our belief that a key step in the growth process is the genesis of the primary embryo and the model of its growth for specific developmental situations. The observed structure at all levels is a silicified record of what happens at the growing margins involving the accretion of surfactant–silicate micelles by a critical size surfactant–silicate embryo. The proposed shape and pattern forming model for mesoporous silica is considered to involve a non-linear dynamical growth scheme incorporating activation and inhibition feedback processes.[1,10] A surfactant–silicate site located in the seed is anticipated to promote the accretion of its own kind from solution to form polymerized mesoporous silica at the same location. The formation of this new and less reactive state of silica from silicate could inhibit the subsequent deposition and accumulation of surfactant–silicate solute at this growth front. Other activators and inhibitors could also contribute to this growth scheme. For instance, the formation of Si—O—Si bonds through elimination of water from the condensation-polymerization of adjacent Si—OH silicate hydroxy groups is expected to be exothermic. This process is expected to cause a local rise in temperature which will promote the rate that silicate transforms to silica at this region of the surfactant–silicate embryo. The simultaneous production of water that occurs during this thermal activation event will, however, be damped by the decrease in the local concentration of solute and the increase of the pH. These changes will both serve to inhibit the rate of deposition and polymerization of surfactant–silicate solute species at the point of impact with the embryonic assembly. Accompanying the silicate to silica transformation is a local tightening-up of the system which results in contraction induced linear and torsional stresses that can be relieved by the system undergoing local bending and twisting distortions. The above processes likely contribute to the curved forms of the mesoporous silica morphologies that evolve in three spatial dimensions.[10] It is interesting to consider that specific kinds of microscopic defects that may exist in the silicate liquid-crystal seed could set the stage for the growth of a particular morphology, for instance a screw dislocation could lead to mesoporous silica spiral shapes.[8,10,12]

Relation between mesoporous silica morphologies and channel patterns grown in two and three spatial dimensions

With the information for the growth and form of mesoporous silica in solution, it is proposed that a surface-confined silicate liquid-crystal embryo is likely involved in a similar kind of polymerization and growth process. What differentiates the growth scenarios in two and three spatial dimensions is the anisotropy of the surface compared to the isotropy of the solution process. The embryo is constrained to grow in two spatial dimensions at the boundary between air and water whereas it is free to grow in all three spatial dimensions in solution. Proximity effects arising from growth fronts of neighboring nuclei are also expected to have a greater influence on the growth process occurring in the surface than in solution.

Finally, the anticipated existence of microscopic defects and associated distortions in the director field of the emerging silicate liquid crystal are likely to contribute to the channel patterns of the silicified film.[8,12]

Relation to stripe domain patterns found in modulated phases in physical and chemical systems

An optical micrograph of a mesoporous silica film grown at the air/water interface serves to emphasize micrometer-scale stripe-like domain patterns running throughout the area of the film, Fig. 4. The resemblance of these patterns to those of modulated stripe phases is intriguing. The latter are pervasive in diverse physical and chemical systems, exemplified by type I superconducting films in an intermediate equilibrium state, far from equilibrium reaction–diffusion Turing chemical patterns, magnetic domain structure of garnets and ferrofluids, and phase separated decorations of diblock copolymers and compressed Langmuir films.[11] Clearly there is a superficial likeness between the stripe patterns of the mesoporous silica films and those found for various modulated phases. However, one must question whether or not there are any similarities between the physicochemical interactions in these systems that could be responsible for the emergence of these characteristic designs.

The length scales of the structural features in documented stripe patterns can vary from mesoscopic to macroscopic dimensions.[11] The stability of these phases is thought to originate from competing interactions and is manifest as periodic spatial variations of an order parameter (e.g., magnetization, polarization) that appear as inhomogeneities in an otherwise uniform system. Pertinent to the observation of channel patterns in mesoporous silica films is the case of Langmuir films of insoluble amphiphilic layers adsorbed at the air/water interface. Associated with the polar head-groups of these amphiphiles is a permanent, or induced, electric dipole moment. Compression of these Langmuir monolayers first creates electrically charged two-dimensional bubble domains. Repulsive interactions between these circular domains cause them to become organized into regular patterns. As the strength of the electrostatic repulsion between domains is increased, through further compression of the Langmuir film, the bubbles are observed to deform into elongated shapes which organize into a stripe phase.[11]

Inspection of the optical micrograph shown in Fig. 4 reveals stripe-like patterns in the mesoporous silica film which appear to be characteristic of the evolution of a system of domains that mutually repel one another; that is, a type of frustration. This raises the possibility that in the formation of a mesoporous silica film, there exists an interplay between packing effects of a silicate liquid-crystal seed constrained to polymerize and grow in two spatial dimensions, subject to electrostatic repulsions between charged domains, and spatio-temporal dynamical effects arising from reaction–diffusion in a non-equilibrium chemical system. Together, these physical and chemical effects could yield the observed stripe-like domain pattern.

Stress in mesoporous films

The sol–gel process, in its broadest terms, refers to the preparation of ceramic materials through the synthesis of a sol, gelation of the sol, and removal of the solvent. The materials produced are often porous and the process of drying can cause the development of stress, which can lead to deleterious warping and cracking effects.[13] In brief, shrinkage of sol–gel derived porous silica that occurs during the evaporation of imbibed water originates from capillary stresses. It is capillary tension associated with solid/water and air/water interfaces in the pore network that creates stress fracture. Reduction of the tension in the network can be achieved by any method that serves to either strengthen the network, such as aging, or decreasing the capillary pressure, such as increasing the pore size and lowering the surface tension. The latter is typically achieved through the use of surfactant additives, supercritical drying and freeze drying.[13]

The synthesis of a mesoporous silica film at the air/water interface can be viewed as a surfactant-templated sol–gel surface-confined process. Because of the high curvature of the mesopores one might expect, by comparison with conventional sol–gel derived porous silica, that these films would be exceptionally susceptible to fracture during drying. That this is not always the case implies that there may be different factors responsible for stress development in mesoporous silica films. In contrast to sol–gel derived silicas with their typically broad pore size distribution, the surfactant-templated mesoporous silicas have pores that are essentially monodisperse. This is expected to lead to a reduction in differential capillary tension between pores and less stress in the mesoporous silica film. Additionally, the mesopores are essentially filled with surfactant micellar structures, together with small amounts of water of hydration located between the head-groups and the silica channel walls. The surfactants serve therefore to reduce the interfacial energy and hence the capillary stress in the mesoporous silica making it less likely to fracture than a conventional sol–gel derived silica.

In the case of mica and graphite, strong interfacial interactions and differences in the lattice dimensions between the substrate and the deposited mesoporous silica create stresses in the boundary region, which lead to micrometer dimension crack patterns in the film.[14,15] By comparison, the mesoporous silica films synthesized at the air/water interface are devoid of cracks; however, they are contorted into intriguing micrometer-scale hillock-like forms outwardly protruding from the surface of the film, Fig. 5 and 6.

The interfacial tensions existing at the boundary between air and water, where the mesoporous silica film grows, are expected to be weak by comparison with mica, thereby decreasing the stresses and reducing the probability of fracture of the film. However, the extensively curved channels that meander throughout the films grown at the air/water interface, Fig. 2, are expected to generate radial stresses through the differential contraction of the silica channel walls, between the top and bottom surface of the film, induced by the silicate condensation–polymerization process. The tension in the film can therefore best be relieved by warping to produce the observed pattern of curvilinear shapes.

A simple 'radial-stress' model can reasonably explain the emergence and form of the protuberances. The basic assumption involves the lower temperature and acidity expected at the air/water interface, causing the rate of polymerization of the silicate precursor to be slower at the top surface of the film compared to the bottom. Thus an increasing rate of polymerization with distance from the top surface is expected to result in differential contraction of the channel walls with depth in the mesoporous silica film. Moreover, because of the channel patterns in the film, this will ensure that the bending will create the observed protuberances. Consider a time slice for the case of an initially flat film. In what follows we calculate the difference in contraction as a function of depth into the film. In Fig. 7(A) a sketch is presented of the contraction and bending of the film. An enlarged view of two neighboring layers that have contracted at different rates is shown in Fig. 7(B). Introducing a coefficient of contraction β as the ratio between the new and old linear dimensions, one can find that the angle of bending α is given by:

$$\sin\alpha(h) = \frac{R_{new}(h) - R_{new}(h+dh)}{dh} = R_{old}\frac{d\beta}{dh}$$

We will treat R_{old} as constant during the silicate polymerization and equal to some definite radius at the top of the film. Even

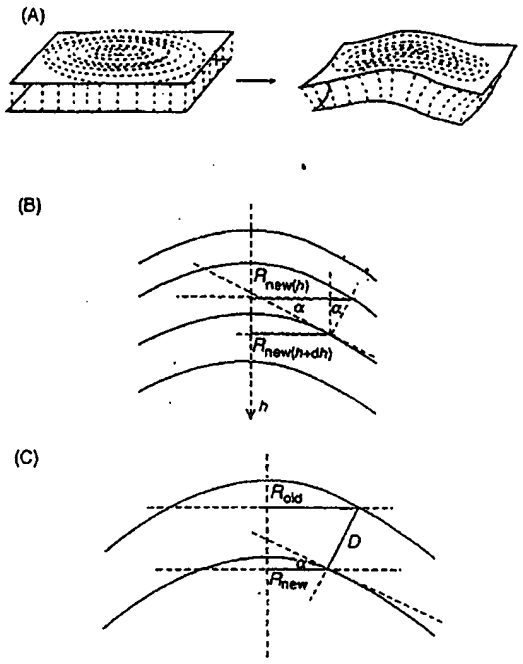

Fig. 7 (A) A sketch of the film contraction induced by radial stress, (B) variable degrees of bending inside the film due to differential radial stresses, and (C) uniform bending of the entire thickness of the film for the linear contraction model

though the radii on the top are expected to show some change, the above condition is still valid because the bending is determined by the relative change of the radius. If the derivative of the contraction coefficient β with respect to the depth h is a constant, that is, an assumed linear change of contraction, then the film will bend without internal torsion. The surface of such a warped film should be rather smooth and round. This appears to be the case in our measurements, excluding however the slight angular-shaped tips of some of the protuberances, Fig. 5(A). From underneath, the mounds look quite round, Fig. 5(B). This implies that the linear model is quite good, except for the section near the top of the mound corresponding to the very early stage of the film growth.

Let us now analyze the 'linearity parameter' of this model, based on the AFM topology measurements. A linear contraction coefficient β with respect to the depth h implies:

$$\beta = 1 + \chi h/D$$

where h is the depth in the film ($h=0$ at the top of the film), χ is the linearity parameter, D is the thickness of the film (introduced to make the parameter χ dimensionless). A 'normalization condition' was employed, which implies that no contraction occurs on the top of the film, which means that only the relative contraction plays a role, and the top is the point of origin. From Fig. 7(C), one finds that:

$$\sin(\alpha) = \frac{R_{new}}{D}\left(\frac{1}{1+\chi} - 1\right)$$

where R_{new} is the radius of the film with respect to the center of the mound of interest. From the AFM measurements, the estimated average thickness of the film $D \approx 530$ nm. Collecting the values of R_{new} and the corresponding angles α, one obtains the linearity parameter χ. This measument was conducted for 46 different radii and mounds, to obtain a histogram for the linearity parameter χ, Fig. 8. The results provides evidence that the linear radial contraction model can explain the shapes of the mounds quite well with $\chi \approx -0.06$. Some deviation from

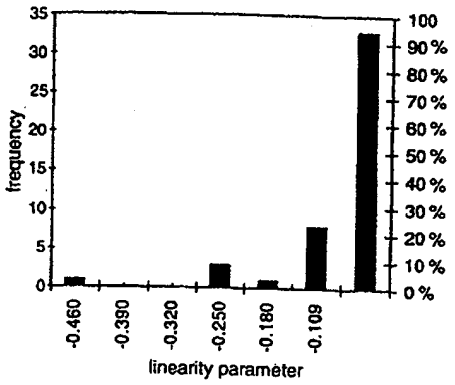

Fig. 8 Histogram of the linearity parameter χ in the radial stress model for the curvature of a mesoporous silica film synthesized at the air/water interface

the linear model, seen in the histogram, could originate from non-radial channel patterns and intrinsic defects within the film. A representative triangular shaped defect in the film is depicted in Fig. 9 which might be responsible for the deviations from the linear contraction model.

Is the linear radial stress model the only source of the surface patterns? Control experiments have been performed with as-synthesized films prepared at room temperature and 80 °C, as well as with wet films and films that had been allowed to dry in ambient air. The hillocks appear in both the room temperature and 80 °C film preparations, and moreover originate during the film growth rather than the drying process. There are no indications that adventitious particulates in the synthesis system contribute to the formation of the mounds observed in the films, as the top and bottom surfaces of the films appear to be devoid of particles, as judged by AFM, SEM and LSCM imaging methods. Also, bubbles do not appear to be involved in the creation of the mounds. First, the growth fronts corresponding to the underneath surface of the films, within the mounds and on the plateau regions, have comparable microroughness, which would not be the case if the atomically smooth surface of the bubble interface had contributed. Second, there is no evidence for occluded bubbles within the films. Interestingly, the protuberances prefer to emerge orthogonally from the film into the air rather than into the water phase. Importantly, the wall thickness of the film remains the same within 20% in the deformed and undeformed regions. The direction of bending might derive from repulsive interactions at the interface between the mesoporous silica film and the aqueous phase. Presumably an

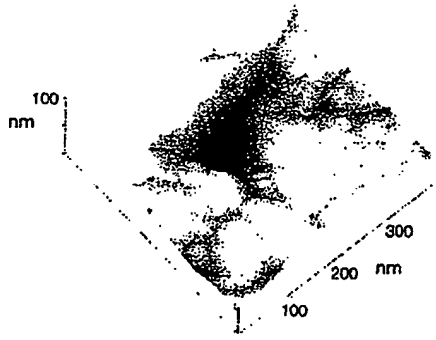

Fig. 9 AFM image of an intrinsic triangular shaped defect on the growing lower side of a mesoporous silica film synthesized at the air/water interface

outward bending motion of the film into the air rather than into the water, is also a lower energy elastic deformational pathway. Together, these control experiments imply that warp patterning of the films is intrinsic to the growth rather than the drying process.

Thermal properties of mesoporous films

To investigate the effect of this unusual channel architecture on the removal of the surfactant template and the thermal stability of the mesostructure, an *in situ* variable-temperature PXRD study of the free-standing mesoporous silica film was conducted in air. Fig. 10.

The results demonstrate that the channel structure is retained to at least 650 °C and begins to collapse at 850–900 °C. As expected, the (100) reflection shifts to slightly higher angles during the template removal procedure because of the thermally induced shrinkage of the hexagonal unit cell arising from the condensation of residual Q^3 to Q^4 groups in the silica channels. It is worth noting that the splitting and broadening observed for the (100, 200) PXRD reflections might arise from differences in the channel center-to-center distance that are expected to originate from the radial stress induced distortion of the film.

Conclusion

Mesoporous silica films synthesized at the air/water interface show unusual surface designs and channel patterns originating from a unique kind of growth process. Channel patterns basically comprise concentric circles, herringbones, fingerprints and hairpins. It is suggested that these patterns are spatio-temporal silicified recordings of the polymerization and growth of a silicate liquid-crystal seed emerging in two spatial dimensions at the air/water interface. Defects that are expected to exist in a surface confined precursor silicate liquid-crystal film will likely cause distortions in the director field and create a liquid-crystalline texture in the resulting mesoporous silica film. There may be a connection between the channel patterns in mesoporous silica films and the stripe domain patterns found in modulated phases. The channel patterns in the surface grown films seem to be two-dimensional renditions of the channel plans found in three-dimensional morphologies,[10] where the anisotropy of surface growth and frustration effects arising from neighboring growth centers, are replaced by the isotropy of the solution growth process. Polymerization induced radial stresses produced in the mesoporous silica film can be released through warping of the film into micrometer-scale hillock protuberances. These are arranged in patterns that appear to reflect the channel curvature designs within the film. A linear radial stress model successfully accounts for the warp patterns observed in the mesoporous silica films.

Financial support from Mobil Technology Company is highly appreciated. H.Y. is grateful for an Ontario Graduate Scholarship and a University of Toronto Open Fellowship held during this research. Use of the LSCM in the Ontario Laser Lightwave Research Centre and the AFM in the laboratory of Professor Grant S. Henderson is deeply acknowledged. Technical discussions with Professor Raymond Kapral proved to be most valuable.

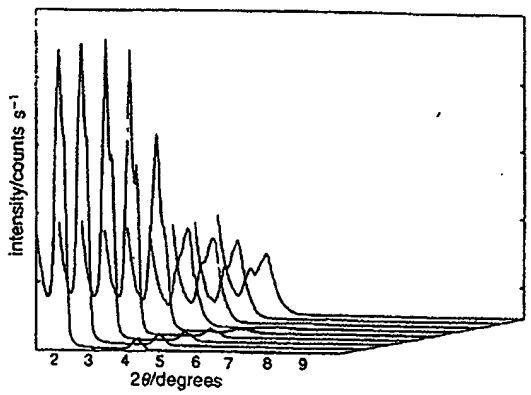

Fig. 10 *In situ* VT-PXRD patterns of a mesoporous silica film grown at the air/water interface. The temperatures starting from the left-side of the traces are 450 (1.75 h), 500, 650, 700, 750 (25 min), 750 (50 min), 750 (2 h), 750 (3.5 h), and 800 °C, respectively, where the numbers in parentheses represent the time that the sample was held at each temperature.

References

1 *Chemical Waves and Patterns*, ed. R. Kapral and K. Showalter, Kluwer Academic Publishers, Dordrecht, 1995.
2 C. T. Kresge, M. E. Leonowicz, W. J. Roth, J. C. Vartuli and J. C. Beck, *Nature (London)*, 1992, 359, 710.
3 H. Yang, N. Coombs, I. Sokolov and G. A. Ozin, *Nature (London)*, 1996, 381, 589.
4 J. Böcker, M. Schlenkrich, P. Bopp and J. Brickmann, *J. Phys. Chem.*, 1992, 96, 9915.
5 J. R. Lu, Z. X. Li, J. Smallwood, R.K. Thomas and J. Penfold, *J. Phys. Chem.*, 1995, 99, 8233.
6 R. K. Thomas and J. Penfold, *Curr. Opinion Colloid Interface Sci.*, 1996, 1, 23.
7 O. Regev, *Langmuir*, 1996, 12, 4940.
8 D. Demus and L. Richter, *Textures of Liquid Crystals*, Verlag Chemie, Weinheim, 1978.
9 Y. S. Lee, D. Surjadi and J. F. Rathman, *Langmuir*, 1996, 12, 6202.
10 H. Yang, N. Coombs and G. A. Ozin, *Nature (London)*, 1997, 386, 692; G. A. Ozin, H. Yang, N. Coombs and I. Sokolov, *Adv. Mater.*, 1997, 9, 662.
11 M. Seul and D. Andelman, *Science*, 1995, 267, 476.
12 *Pattern Formation in Liquid Crystals*, ed. A. Buka and L. Kramer, Springer, New York, 1996.
13 C. J. Brinker and G. W. Scherer, *Sol–Gel Science, The Physics and Chemistry of Sol–Gel Processing*, Academic Press, San Diego, California, 1990.
14 H. Yang, A. Kuperman, N. Coombs, S. Mamiche-Afara and G. A. Ozin, *Nature (London)*, 1996, 379, 703.
15 H. Yang, N. Coombs, I. Sokolov and G. A. Ozin, *J. Mater. Chem.*, 1997, 7, 1285.

Paper 7/02110K; *Received* 26*th March*, 1997

Exhibit 3

Mesostructured Silica Formed on the PI-2 Film

PI-2

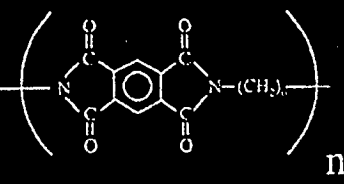

Optical Micrograph

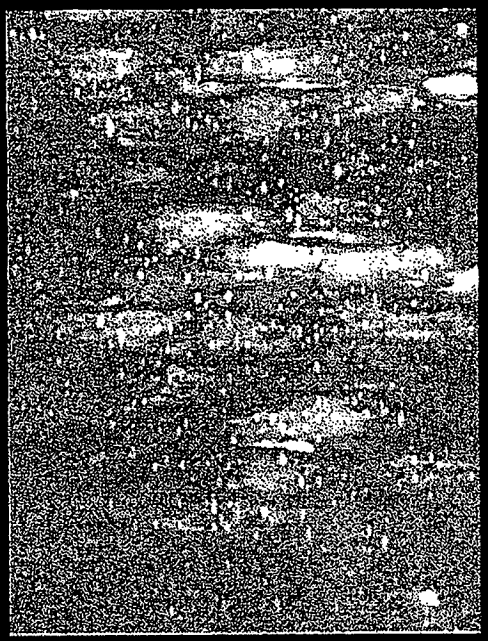

↑ Rubbing ×1000

In-Plane XRD

ϕ-2$\theta\chi$ scan

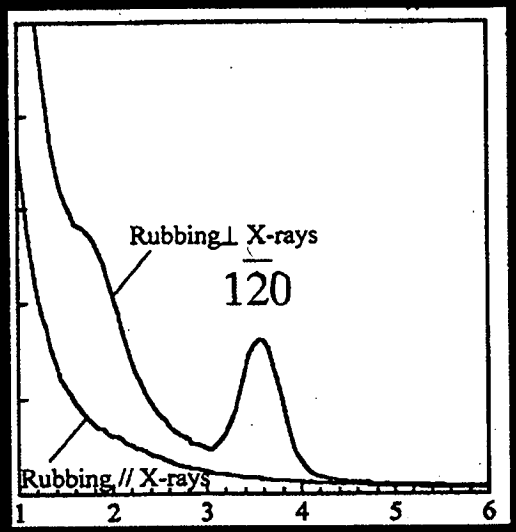

ϕ scan

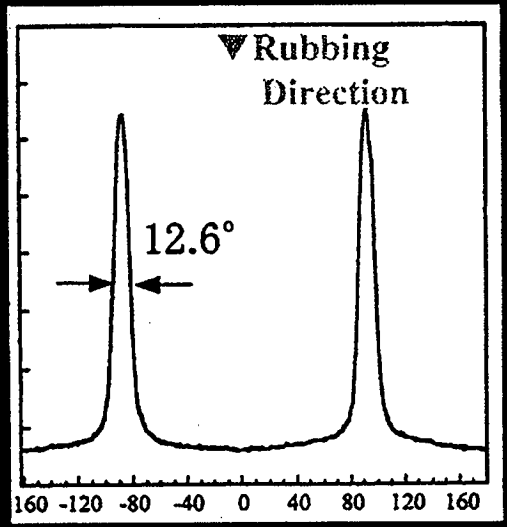

Mesochannels ⊥ Rubbing Direction
Fine Uniaxial Alignment
Transparent Continuous Film

EXHIBIT 4

X-ray Diffraction Experiments

Conventional θ–2θ Scanning

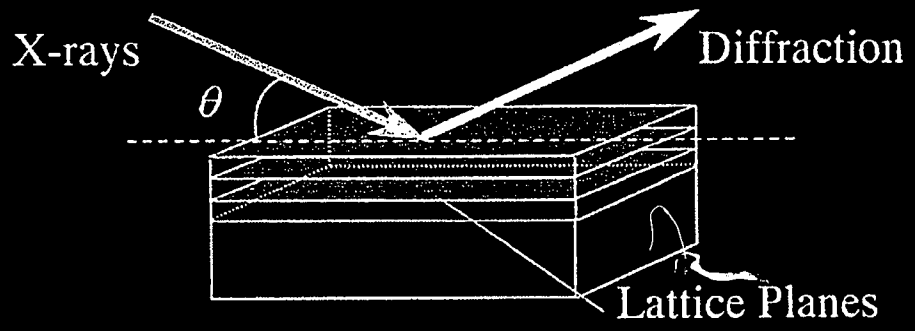

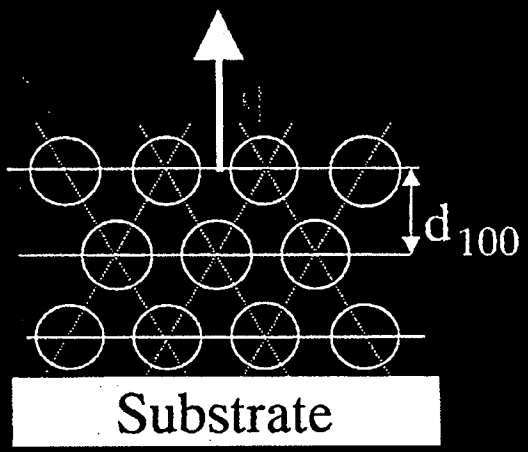

In-Plane Diffraction